

# Quantum Dots, Part 1: Optical and Electrochemical Properties of CdTe Quantum Dots

A. Habekost\*

University of Education Ludwigsburg, Department of Chemistry, Reuteallee 46, D-71634 Ludwigsburg, Germany

\*Corresponding author: A.Habekost@t-online.de

**Abstract** Quantum dots (QDs) are colloidal semiconductor clusters with physical dimensions in the range of several nanometers. Since the discovery of QDs in 1983, there has been a wide variety of research interest and activity. In particular, the mechanisms behind photoluminescence (PL) and electrogenerated chemiluminescence (ECL) and the applications of QDs have been extensively investigated. Bright fluorescence effect many analytical and technical applications: QDs have found promising applications as fluorescent biolabels [1,2], in optoelectronic and photovoltaic devices [3,4], and in light-emitting diodes (LEDs) [5,6]. This paper outlines some straightforward electrochemical and spectroscopic experiments with commercial CdTe QDs to explain their background mechanisms (e.g., electron-hole separation and recombination).

**Keywords:** *three-year undergraduate, quantum dots, electrochemistry, electrochemiluminescence, UV-VIS-spectrometry, hands-on learning/manipulatives*

**Cite This Article:** A. Habekost, "Quantum Dots, Part 1: Optical and Electrochemical Properties of CdTe Quantum Dots." *World Journal of Chemical Education*, vol. 5, no. 4 (2017): 120-127. doi: 10.12691/wjce-5-4-1.

## 1. Introduction

Colloidal nanocrystals, called quantum dots, are clusters with physical dimensions in the range of several nanometers. In 1983, Brus et al. [7] were the first to report size effects in the excited state of small, crystalline CdS particles. The authors described photophysical and electrochemical experiments with CdS particles on the basis of electron ( $e^-$ ) - hole ( $h^+$ ) separation (excitons) and their recombination. This  $e^-$  -  $h^+$  recombination causes luminescence in the visible region and makes CdS QDs into a powerful optical device. Valence and conduction band energies can be related to the electrochemical redox potential, allowing the redox potential to be assigned to  $e^-$  and  $h^+$ . In CdS nanoparticles, these values are -0.7 V and +1.7 V (vs. NHE), respectively. In subsequent papers, Brus calculated the size-dependence of the  $e^-$ - $h^+$  redox potential and the electron energy of the lowest excited state as a function of the crystallite diameter for ZnO, CdS, GaAs and InSb [8,9]. Baskoutas and Terzis used different theoretical approaches to calculate the size-dependent band gap of various QDs [10]. In a bulk semiconductor the electrons and holes move freely throughout the crystal. In a nanocrystal, however, quantum-confinement restricts this motion and lead to a variety of optical and electronic consequences, i.e. the size-dependent band gap. Therefore, the band gap in the QDs is increased compared to the band gap in the semiconductor.

In the following years, most publications focused on investigating the experimental and theoretical background of QDs in detail [11]. Baker and Baker [12] summarized recent investigations about the synthesis, characterization

and application of carbon nanodots (C-dots), another type of QD. These C-dots typically contain carboxylate moieties on their surface, thus giving them excellent water solubility. C-dots are a good supplement for single or multi-walled carbon nanotubes or other nanocarbons such as fullerene or nanodiamonds. Omer and Bard [13] reported the preparation, characterization, and electrogenerated chemiluminescence (ECL) of aromatic hydrocarbon nanoparticles in aqueous solution. ECL was observed in aqueous tripropylamine /  $\text{NaClO}_4$  solution.

Figure 1 shows a comparison between the two principle spectral and electrochemical processes that can explain the spectral emission of QDs: photoluminescence (PL) and electrogenerated chemiluminescence (ECL). In PL, the incident light transfers an electron from the valence bond (VB) to the conducting band (CB) of the QD core, and an  $e^-$ - $h^+$  separation occurs. The band gap between VB and CB depends on the QD and lies between 1 and 3 eV [11]. This band gap can be estimated from the center of the PL spectra. Surface states may play an important role in QD spectroscopy, because the size of a QD is small compared to its surface. On the surface of QDs, chemical bonds are disrupted, and these non-coordinative bonds (often called dangling bonds) can capture electrons or holes. This is known as a surface trap. The trapped electrons can thermalize via a radiative transition to the surface ground state ( $h\nu_2$ ) or a non-radiative transition to VB (see the dotted lines in Figure 1, left). This surface route leads to a broadening or to a red shift of the PL spectra. The electrons migrate from the core CB over the surface states to the core VB. In addition, the surface states can act as a quencher for PL followed by a significant decrease in PL intensity.

At first glance, ECL is analogue to PL. But in ECL, the electrons primarily come from the electrode. The potential

of the electrode is a good means to scan the electron energy: Applying a (negative) potential, the surface states are initially filled with electrons (Figure 1, right). On increasing the potential, the electrons can occupy the CB states, too. In ECL, the coreactants play an important role. To understand this, a distinction must be drawn between reductive-oxidative (RO, sometimes called cathodic) and

oxidative-reductive (OR, called anodic) ECL. In the first process, an electron from the electrode occupies an excited surface or a CB state. Another electron from the electrode interacts with the coreactants (co) to form a radical cation ( $co^{\cdot+}$ ). The resulting hole occupies a surface state or is injected into a VB state. Therefore, an  $e^- - h^+$  pair results that can emit radiation (see Figure 2).

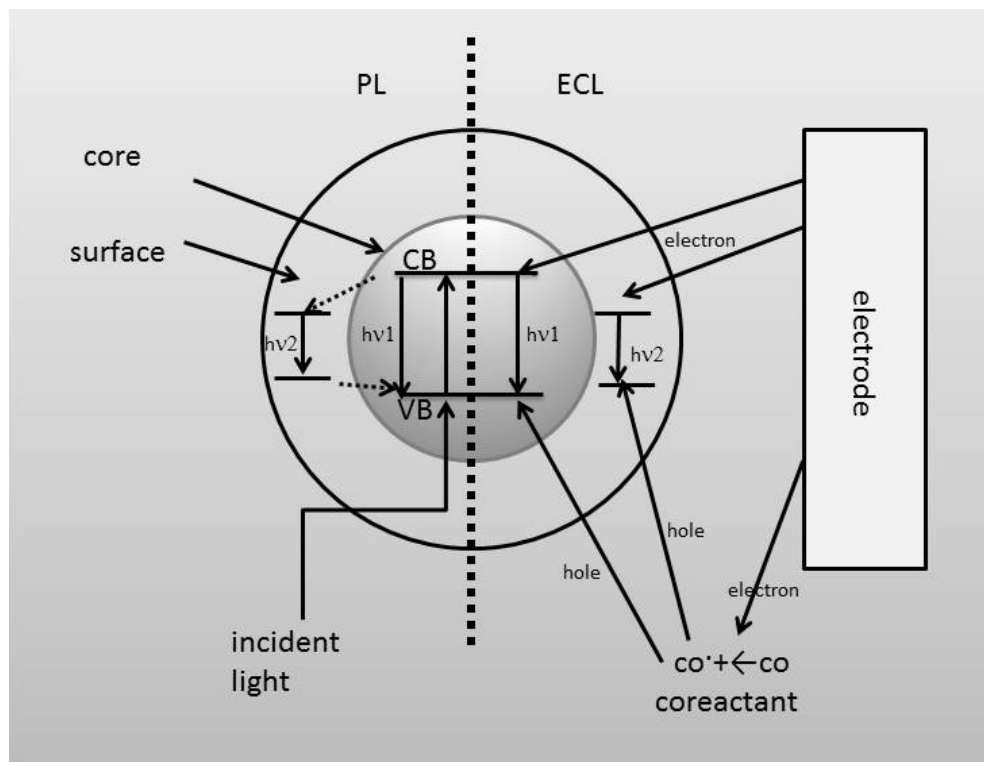


Figure 1. Schematic comparison of PL and ECL mechanisms of QD

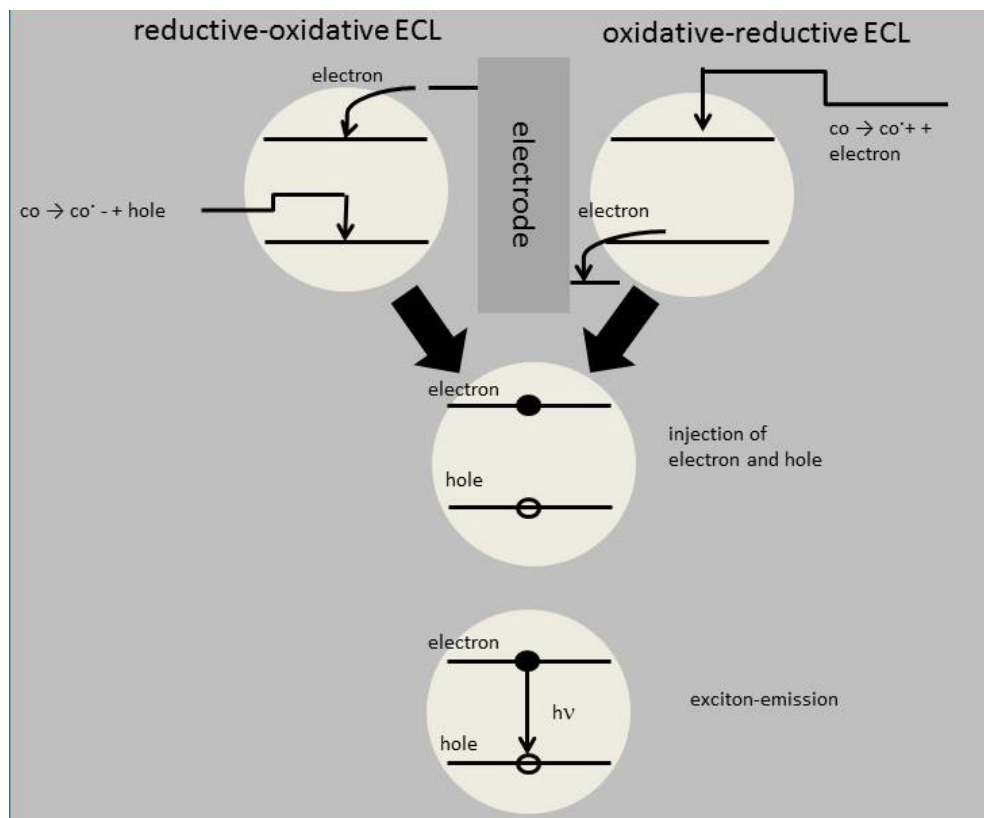
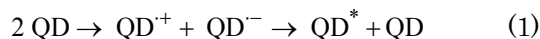


Figure 2. Details of the RO and OR processes, after [11]

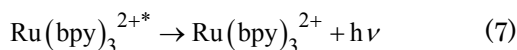
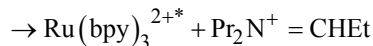
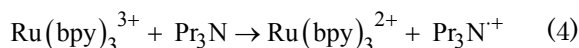
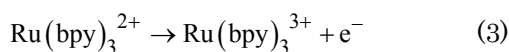
In the OR-ECL process, the coreactants are electrochemically oxidized, and the resulting electron occupies the CB of the QDs. Simultaneously, an electron from the VB fills an electrode state. Overall, an  $e^- - h^+$  pair results similarly to in the RO mechanism.

Besides the different excitation mechanisms, PL and ECL differ regarding the coreactants that are necessary for ECL. Although the QD itself can undergo a redox reaction, this so-called annihilation-type ECL (see eq. 1 and 2) often plays a minor role if coreactants are present.



Typical coreactants for the RO-mechanism are  $\text{O}_2$  [14Zou, Ju],  $\text{H}_2\text{O}_2$  [15,16],  $\text{S}_2\text{O}_8^{2-}$  [17], and for the OR-mechanism these coreactants are tripropylamine (TPA), dibutylammonioethanol (DBAE) [18,19],  $\text{C}_2\text{O}_4^{2-}$  [20], and proline [21].

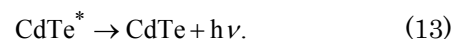
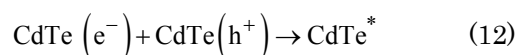
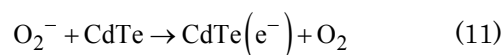
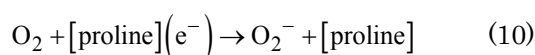
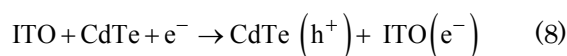
In case of the OR-mechanism, the reaction scheme is quite similar to those of the well-known ECL-reaction of  $\text{Ru}(\text{bpy})_3^{2+}$ , here illustrated with the most commonly used coreactant, tripropylamine ( $\text{Pr}_3\text{N}$ ), eq. 3-7 [22].



(Pr: propyl, Et: ethyl,  $h\nu$ : energy of the emitted light).

Reaction (3) may be an electrode process or a direct oxidation with an oxidizing agent. In contrast to the above scheme, there may also be a direct oxidation of  $\text{Pr}_3\text{N}$  (sometimes as a competition process).  $\text{Ru}(\text{bpy})_3^{2+}$  reacts with the  $\text{Pr}_2\text{NC} \cdot \text{HEt}$  radical to form  $\text{Ru}(\text{bpy})_3^{2+*}$ , a species in an excited state that undergoes radiative decay. In addition, eq. (5) shows that the formation of  $\text{Ru}(\text{bpy})_3^{2+*}$  and subsequent emission of light is pH-dependent. An analogous mechanism results when  $\text{Ru}(\text{bpy})_3^{2+}$  is replaced with QDs (see eq. 4 – 6).

Both CdTe [23,24] and CdSe [25] were found to be efficient ECL emitters on indium-tin oxide (ITO) electrodes with proline as coreactants [21]. As can be seen from eq. 4 – 6, the coreactant is strongly involved into the ECL process. Zhang et al. [21] proposed the following mechanism to explain the ECL of the ITO / CdTe / proline ternary system.



The formation of a  $\text{CdTe}^*$  radical anion involves the electrode,  $\text{O}_2$ , and proline: The electron transfer starts at the ITO. This results in a hole in the VB of CdTe (eq. (8)). Simultaneously, proline reacts in an alkaline medium with  $\text{O}_2$  forming an  $\text{O}_2^-$  anion. The redox reaction between  $\text{O}_2^-$  and CdTe pumps an electron into the CB of CdTe. Subsequently,  $\text{CdTe}(e^-)$  and  $\text{CdTe}(h^+)$  annihilate and form  $\text{CdTe}^*$  in an excited state, which decays by emitting radiation. The authors constructed a flow cell to quantitatively determine proline in a concentration range between  $1.0 \cdot 10^{-8} - 1.0 \cdot 10^{-4}$  g/mL. There have been some other reports on the ECL of  $\text{Ru}(\text{bpy})_3^{2+}$  resp. QDs and proline [21,22].

Recent didactic publications paid particular attention to the synthesis and optical characterization of QDs [26-29], the comparison of QDs with fluorescing dyes [30], and quantum confinement effects of QDs [31]. The direct relationship between size and spectral distribution of QD fluorescence implies that optical tunability can be easily controlled. QDs show this size-dependence if the size of the QDs is less than the exciton Bohr radius,  $r_B$  (14).

$$r_B = h^2 / 4\pi^2 \epsilon \epsilon_0 / e^2 \left( \frac{1}{m_e^{\text{eff}}} - \frac{1}{m_h^{\text{eff}}} \right), \quad (14)$$

where  $m_e^{\text{eff}}$  and  $m_h^{\text{eff}}$  are the effective mass of the electron and hole, respectively,  $e$  is the elementary charge,  $h$  is Planck's constant, and  $\epsilon$  and  $\epsilon_0$  are the dielectric constant and vacuum permittivity, respectively.

For instance, the Bohr radii of ZnS, CdS, and CdTe are 2.2 nm, 2.4 nm and 7.5 nm, respectively [32]. Due to dielectric screening, the effective mass of electron and hole are smaller than that of the free electron.

The quantum mechanical particle in a box concept shows that as the size of the nanocrystal increases both the absorption and emission shift to higher wavelengths [33]. Therefore, the emission of white light is possible by mixing QDs with different particle size. Figure 3 illustrates the size-dependent energy gap between CB and VB.

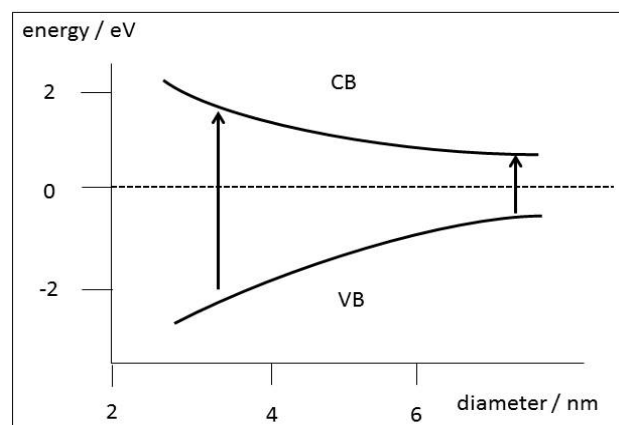


Figure 3. Schematic representation of the size-dependent band gap

The band gap energy can be calculated according to eq. 15 [31]:

$$E_{BG} = E_{BG}^{bulk} + \frac{h^2}{8R^2} \left( \frac{1}{m_e^{eff}} - \frac{1}{m_h^{eff}} \right) - \frac{1.8e^2}{4\pi^2 \epsilon \epsilon_0 e R}, \quad (15)$$

where  $R$  is the radius of the nanocrystal and  $E_{BG}^{bulk}$  is the band gap energy of the bulk semiconductor.

Because the excited electron and hole attract each other, the band gap energy must be corrected. This stabilization (exciton binding energy) is the correction term (right part in eq. 15).

In this paper we restrict ourselves to experiments that demonstrate the background principles of the spectroscopic and electrochemical behavior of CdTe QDs. The experimental methods employed are UVVIS spectroscopy, linear sweep voltammetry (LSV), and electrogenerated chemiluminescence (ECL). The electrochemical experiments were conducted on an Au screen-printed electrode.

## 2. Experiments

### Hazards (after

[https://en.wikipedia.org/wiki/Cadmium\\_telluride](https://en.wikipedia.org/wiki/Cadmium_telluride))

CdTe is less toxic than elemental cadmium. CdTe has low acute inhalation, oral, and aquatic toxicity. CdTe is not classified as harmful if ingested or if it comes into contact with skin, and the toxicity classification to aquatic life has been reduced. Once properly and securely captured and encapsulated, CdTe may be rendered harmless.

### Chemicals and instruments:

CdTe (Merck, 8258.1, 610 nm), CdTe (Merck, 8260.1, 710 nm),  $\text{Na}_2\text{HPO}_4$  (0.1 mol/L), L-proline (Sigma Aldrich P0380), 2-(Dibutylamino)ethanol (DBAE) (Sigma Aldrich 550035), distilled water.

ECL-Potentiostat (ECLStat, DropSens), screen printed electrodes (DropSens): DS Au-Bt (working electrode (WE): Au, low temperature), SEM in Figure 4)

Luminescence spectrometer (Perkin Elmer LS 50B).

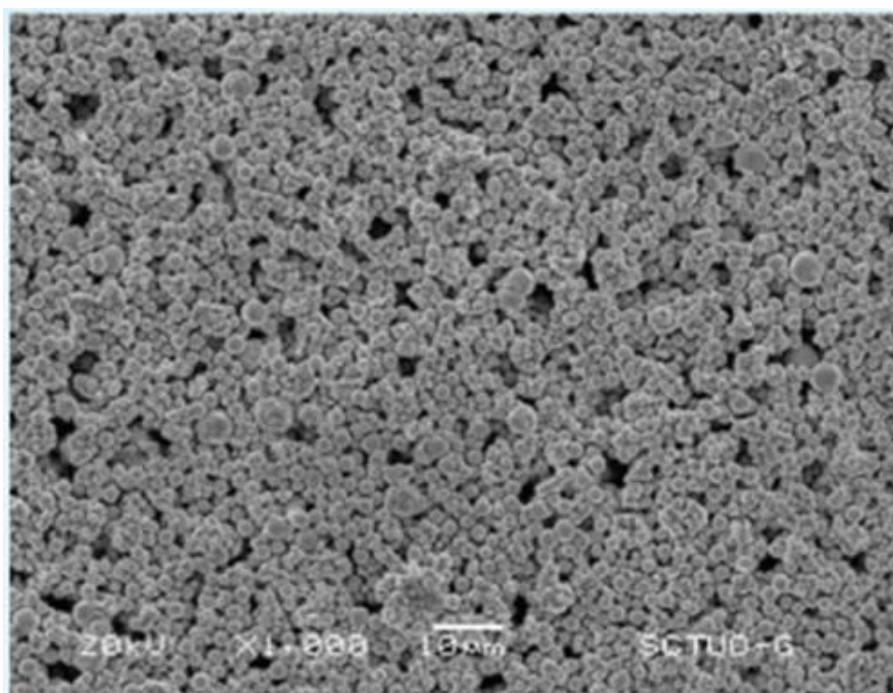


Figure 4. Scanning electron image of Au-Bt (kindly from DropSens)



Figure 5. The CdTe QDs and the aqueous solutions

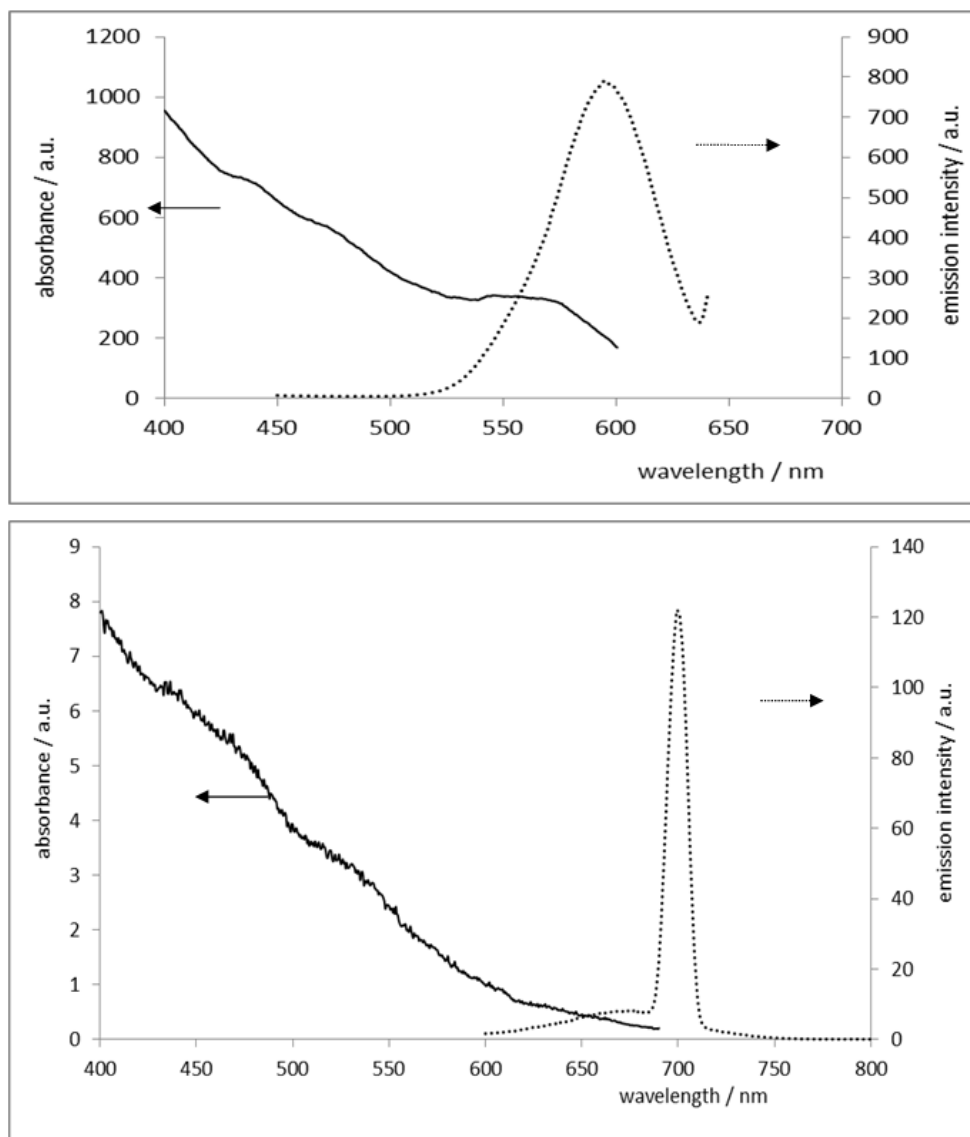


Figure 6. Absorption and emission of 610 nm QDs (top) and 710 nm QDs (bottom)

## 2.1. Spectroscopic Measurements

Figure 5 shows the two CdTe QDs and the aqueous solutions, respectively.

The 610 nm QDs have a band gap of about 2.2 eV, calculated from the absorption peak at 560 nm. This value is shifted to higher energy compared to the band gap of the CdTe bulk (1.5 eV) [35]. The lack of any tail for the PL at longer wavelengths shows, that no significant emission occurs from the surface states. Unfortunately, a pronounced absorption peak for 710 nm QDs is not detectable.

## 2.2. Electrochemical Measurements (CV/LSV – ECL)

Bard's group systematically investigated ECL of CdTe QDs. We summarize only a few results here. The difference between the anodic and cathodic peak in differential pulse voltammetry of TOPO-capped CdTe QDs (TOPO: trioctylphosphineoxide) in dichloromethane, and the absorption peak of about 625 nm reflects the band gap of CdTe QDs of about 2 eV [34]. In addition, a 10 Hz stepping potential was applied between -2.5 V and +1.44

V and a large cathodic ECL was observed. In contrast, a significantly lower ECL intensity occurs if the potential is half-scanned between 0 and -2.5 V. The authors concluded that both a reduced and oxidized form of the QDs must be present to increase the ECL signal. The authors assumed that the coreactant must be the solvent (here  $\text{CH}_2\text{Cl}_2$ ). The same effect was observed in TOPO- and TOP-capped CdSe (TOP: trioctylphosphine) [35]: If the electrode potential was scanned between 0 and +2.3 V the ECL intensity is low, because only oxidized species are formed. In addition, a low ECL intensity results if the potential is scanned between 0 and -2.3 V. However, if the potential is switched between -2.3 V and +2.3 V, the ECL intensity increases significantly.

In our own experiments we saw an analogous effect with proline as coreagent (Figure 7): the ECL intensity increased by a factor of about 7 when the potential scan involved reduced species (reduced  $\text{O}_2$ , scan between -1.8 V and +1.8 V, see the solid lines in Figure 7). The ECL intensity decreased after several scan sequences because proline was electrolytically consumed. The dotted lines reflect the ECL when the potential was scanned between 0 V and +1.8 V.

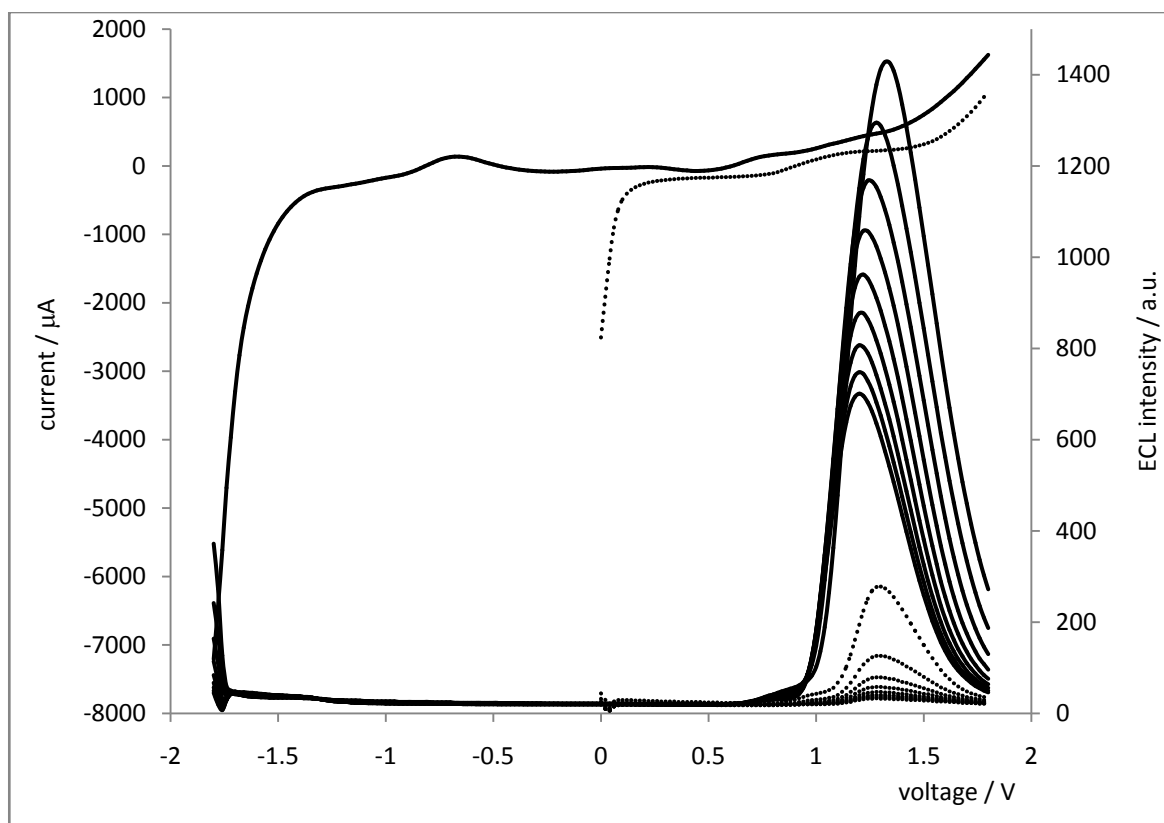


**Figure 7.** LSV and ECL intensity of CdTe / proline at different scan ranges. Solid lines: potential range between -1.8 V and +1. Dotted lines: potential range between 0 and +1.8 V 8 V (nine times in a row, respectively)

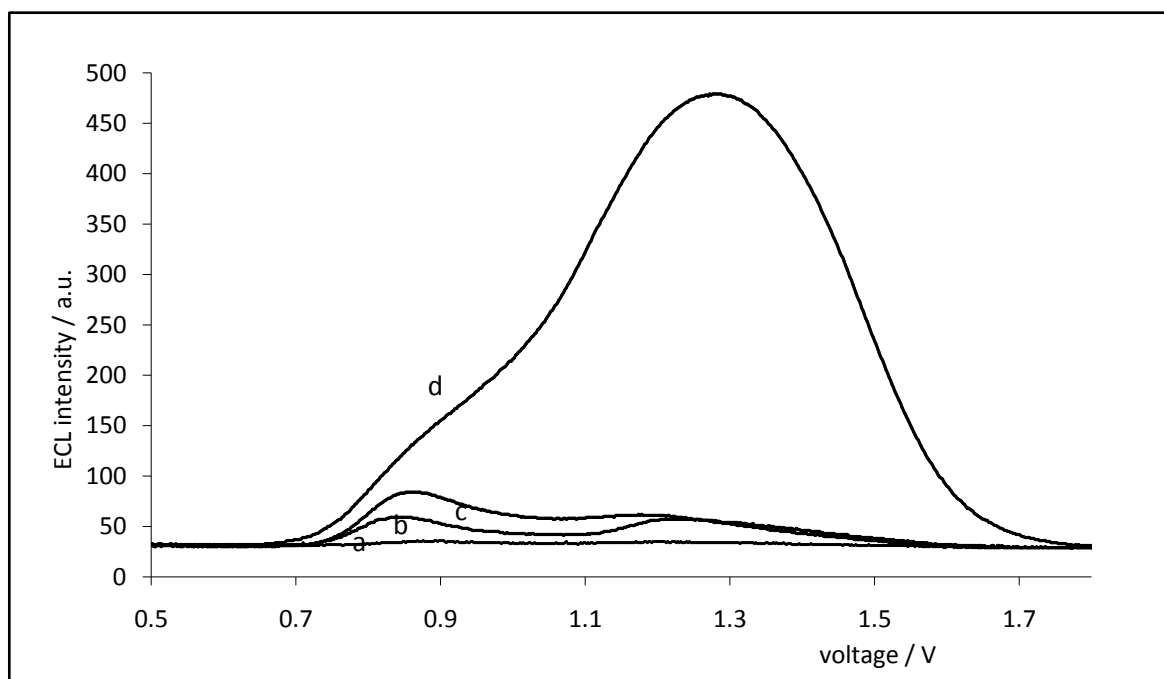
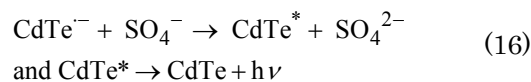


**Figure 8.** ECL intensity with proline and DBAE as coreactants: a) background (without QD), b) with QD (710 nm) and proline, c) as b) with additional QD, and d) as c) with additional DBAE. Insert: detailed representation of the lower ECL signals

### 2.3. LSV of QDs with Proline and with DBAE (OR-mechanism)

The ECL intensity depends on the coreactants used. Figure 8 shows the ECL of a) background, b) QD (710 nm) with proline, c) additional QD, and d) additional DBAE. DBAE as a coreactant is more effective than proline. The

reduction of persulfate produces a strong oxidant,  $\text{SO}_4^{\cdot-}$ , which can subsequently react with the negative charged CdTe QDs by injecting a hole into the VB. This produces an excited state that can emit radiation (see eq. 16).



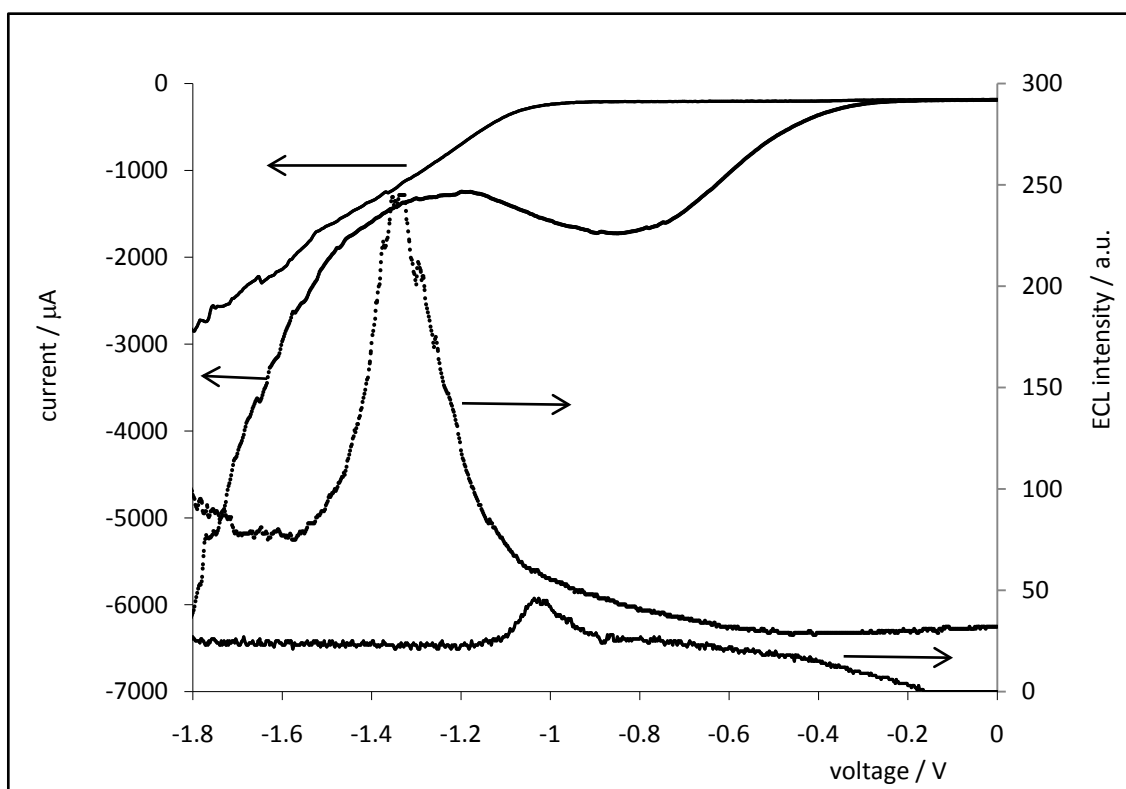


Figure 9. Solid lines: LSV and ECL of QD (710 nm) alone, dotted lines: LSV and ECL of QD (710 nm) and  $K_2S_2O_8$

#### 2.4. LSV of QDs with $K_2S_2O_8$ (RO-mechanism)

Figure 9 shows the LSV and ECL of both QD (710 nm) alone, and with  $K_2S_2O_8$  as coreagent. The coreagent reveals a significantly increased ECL intensity of a factor of about five compared to the ECL of QD alone. In contrast to proline and DBAE,  $K_2S_2O_8$  acts as an oxidative coreagent, which inserts a hole into the VB of CdTe. Simultaneously, an electron from the electrode at negative potential fills the CB (see the left part of Figure 2).

### 3. Conclusion

QDs are growing in significance, especially in technical applications. Therefore, QDs should be a topic in student training.

Conducting QD experiments involves a wide variety of physicochemical principles (voltammetry, spectrophotometry, electrogenerated chemiluminescence). This allows students to see how different analytical methods both supplement and complement each other.

In this paper, we summarized some mechanistic aspects of QDs as well as simple experimental setups to investigate the spectroscopic and electrochemical behavior of CdTe with different coreagents.

### Acknowledgements

A. H. thanks the Vector Foundation (Germany), the Fonds der Chemischen Industrie (Germany), and the Ludwigsburg University of Education for financial support.

### References

- [1] M. Bruchez, M. Moronne, P. Gin, S. Weiss, A.P. Alivisatos, Semiconductor nanocrystals as fluorescent biological labels, *Science* 281, 1033 (1998).
- [2] W.C. Chan, S.M. Nie, Quantum Dot Bioconjugates for Ultrasensitive Nonisotopic Detection, *Science* 281, 1983 (1998).
- [3] D.V. Talapin, J.S. Lee, M.V. Kovalenko, E.V. Shevchenko, Prospects of colloidal nanocrystals for electronic and optoelectronic applications, *Chem. Rev.* 110, 389 (2010).
- [4] P. Bhattacharya, S. Ghosh, A.D. Stiff-Roberts, Quantum dot opto-electronic devices, *Annu. Rev. Mater. Res.* 34, 1 (2004).
- [5] Q.Q. Dai, C.E. Duty, M.Z. Hu, Semiconductor-nanocrystals-based white light-emitting diodes, *Small*, 6, 1577 (2010).
- [6] H.V. Demir, S. Nizamoglu, T. Erdem, E. Mutlugun, N. Gaponik, A. Eychmüller, Quantum dot integrated LEDs using photonic and excitonic color conversion, *Nano Today*, 6, 632 (2011).
- [7] R. Rosetti, S. Nakahara, L.E. Brus, Quantum size effects in the redox potentials, resonance Raman spectra, and electronic spectra of CdS crystallites in aqueous solution, *J. Chem. Phys.* 79, 1086 (1983).
- [8] L.E. Brus, A simple model for the ionization potential, electron affinity, and aqueous redox potentials of small semiconductor crystallites, *J. Chem. Phys.* 79, 5566 (1983).
- [9] L.E. Brus, Electron-electron and electron-hole interactions in small semiconductor crystallites: The size dependence of the lowest excited electronic state, *J. Chem. Phys.* 80, 4403 (1984).
- [10] S. Baskoutas, A.F. Terzis, Size-dependent band gap of colloidal quantum dots, *J. Appl. Phys.* 99, 13708 (2006).
- [11] P. Wu, X. Hou, J.-J. Xu, H.-Y. Chen, Electrochemically Generated versus Photoexcited Luminescence from Semiconductor Nanomaterials: Bridging the Valley between Two Worlds, *Chem. Rev.* 114, 11027 (2014).
- [12] S.N. Baker, G.A. Baker, Luminescent carbon nanodots: Emergent Nanolights, *Angew. Chem. Int. Ed.* 49, 6726 (2010).
- [13] K.M. Omer, A.J. Bard, Electrogenerated Chemiluminescence of Aromatic Hydrocarbon Nanoparticles in an Aqueous Solution, *J. Phys. Chem.* 113, 11575 (2009).
- [14] G.Z. Zou, H.X. Ju, Electrogenerated Chemiluminescence from a CdSe Nanocrystal Film and Its Sensing Application in Aqueous Solution, *Anal. Chem.* 76, 6871 (2004).

- [15] S.N. Ding, J.J. Xu, H.Y. Chen, Enhanced solid-state electrochemiluminescence of CdS nanocrystals composited with carbon nanotubes in H<sub>2</sub>O<sub>2</sub> solution, *Chem. Commun.* 3631 (2006).
- [16] Y.L. Mei, H.S. Wang, Y.F. Li, Z.Y. Pan, W.L. Jia, Enhanced solid-state electrochemiluminescence of CdS nanocrystals composited with carbon nanotubes in H<sub>2</sub>O<sub>2</sub> solution, *Electroanal.* 22, 155 (2010).
- [17] S.K. Poznyak, D.V. Talapin, E.V. Shevchenko, H. Weller, *Quantum Dot Chemiluminescence*, *Nano Lett.* 4, 693 (2004).
- [18] L.H. Zhang, X.Q. Zou, E. Ying, S.J. Dong, Quantum dot electrochemiluminescence in aqueous solution at lower potential and its sensing application, *J. Phys. Chem. C*, 112, 4451 (2008).
- [19] H. Jiang, X.M. Wang, Anodic electrochemiluminescence of CdSe nanoparticles coreacted with tertiary amine and halide induced quenching effect, *Electrochem. Commun.* 11, 1207 (2009).
- [20] Z.F. Ding, B.M. Quinn, S.K. Haram, L.E. Pell, B.A. Korgel, A.J. Bard, Electrochemistry and electrogenerated chemiluminescence from silicon nanocrystal quantum dots, *Science*, 296, 1293 (2002).
- [21] M. Zhang, F. Wan, S. Wang, S. Ge, M. Yan, J. Yu, Determination of L-proline based on anodic electrochemiluminescence of CdTe quantum dots, *J. Lumines.* 132, 938 (2012).
- [22] A. Habekost, Investigations of some reliable electrochemiluminescence systems on the basis of tris(bipyridyl)Ruthenium(II) for HPLC analysis, *World J. Chem. Educ.* 4/1, 13-20 (2016).
- [23] R. Freeman, I. Willner, Optical molecular sensing with semiconductor quantum dots (QDs), *Chem. Soc. Rev.* 41, 4067 (2012).
- [24] M.P. Bruchez, Quantum dots find their stride in single molecule tracking, *Curr. Opin. Chem. Biol.* 15, 775 (2011).
- [25] W. Tu, X. Fan, J. Lou, Z. Dai, Label-free and highly sensitive electrochemiluminescence biosensing using quantum dots/carbon nanotubes in ionic liquid, *Analyst* 140, 2603 (2015).
- [26] M.L. Landry, T.E. Morrell, T.K. Karagounis, C-H. Hsia, C-Y. Wang, Simple Syntheses of CdSe Quantum Dots, *J. Chem. Educ.*, 2014, 91, 274 (2014)].
- [27] L. D. Winkler, J. F. Arceo, W. C. Hughes, B. A. DeGraff and B. H. Augustine, Quantum Dots: An Experiment for Physical or Materials Chemistry, *J. Chem. Educ.* 82, 1700 (2005).
- [28] Y. Pan, Y.R. Li, Y. Zhao, D.L. Akins, Synthesis and Characterization of Quantum Dots: A Case Study Using PbS, *J. Chem. Educ.* 92, 1860 (2015).
- [29] K. J. Nordell, E.M. Boatman, G.C. Lisensky, A Safer, Easier, Faster Synthesis for CdSe Quantum Dot Nanocrystals, *J. Chem. Educ.* 82, 1697 (2005).
- [30] B.M. Hutchins, T.T. Morgan, M.G. Ucak-Astarlioglu, M.E. Williams, Optical Properties of Fluorescent Mixtures: Comparing Quantum Dots to Organic Dyes, *J. Chem. Educ.* 84, 1301 (2007).
- [31] P.J. Reid, B. Fujimoto, D.R. Gamelin, A Simple ZnO Nanocrystal Synthesis Illustrating Three-Dimensional Quantum Confinement, *J. Chem. Educ.* 91, 280 (2014).
- [32] W.E. Buhro, V.L. Colvin, Semiconductor nanocrystals: Shape matters, *Nature Materials* 2, 138 (2003)].
- [33] T. Kippeny, L.A. Swafford, S.J. Rosenthal, Semiconductor Nanocrystals: A Powerful Visual Aid for Introducing the Particle in a Box, *J. Chem. Educ.* 79, 1094 (2002)].
- [34] Y. Bae, N. Myung, A.J. Bard, Electrochemistry and electrogenerated Chemiluminescence of CdTe Nanoparticles, *Nano Lett.* 4, 1153 (2004).
- [35] N. Myung, Z. Ding, A.J. Bard, Electrogenerated Chemiluminescence of CdSe Nanocrystals, *Nano Lett.* 2, 1315 (2002).